# A simple genetic architecture and low constraint allows rapid floral evolution in a diverse and recently radiating plant genus

Jamie L. Kostyun[1,2*], Matthew J.S. Gibson[1], Christian M. King[1,3], and Leonie C. Moyle[1]

[1] Department of Biology, Indiana University, Bloomington, IN 47405

[2] Department of Plant Biology, The University of Vermont, Burlington, VT 05405

[3] Department of Evolution, Ecology and Organismal Biology, The Ohio State University, Columbus, OH 43210

* Corresponding author: Jamie.Kostyun@uvm.edu, Tel: 802-656-7670

**Word count: Summary (200), Introduction (1185), Materials and Methods (1576), Results (1010), Discussion (1821), Acknowledgements (79), Total Main Text (5706), Figures (4, all in color), Tables (2), Supplementary Documents (8 Figures, 7 Tables).**

**Summary**

- Genetic correlations among different components of phenotypes, especially resulting from pleiotropy, can constrain (antagonistic) or facilitate (adaptive) trait evolution. These factors could especially influence the evolution of traits that are functionally integrated, such as those comprising the flower. Indeed, pleiotropy is proposed as a main driver of repeated convergent trait transitions, including the evolution of phenotypically-similar pollinator syndromes.
- We assessed the role of pleiotropy in the differentiation of floral and other reproductive traits between two species—*Jaltomata sinuosa* and *J. umbellata* (Solanaceae)—that have divergent suites of floral traits consistent with bee- and hummingbird-pollination, respectively. To do so, we generated a hybrid population and examined the genetic architecture (trait segregation and QTL distribution) underlying 25 floral and fertility traits.
- We found that most traits had a relatively simple genetic basis (few, predominantly additive, QTL of moderate to large effect), as well as little evidence of antagonistic pleiotropy (few trait correlations and QTL co-localization, particularly between traits of different classes). However, we did detect a potential case of adaptive pleiotropy among floral size and nectar traits.
- These mechanisms may have facilitated the rapid floral trait evolution observed within *Jaltomata*, and may be a common component of rapid phenotypic change more broadly.

46 **Key Words:** floral evolution, genetic co-variation, *Jaltomata*, pleiotropy, Solanaceae,

47 QTL co-localization, QTL mapping

## Introduction

One feature of phenotypic evolution is the broad variation in observed rates of trait change, both among traits within a single lineage and among lineages. How quickly phenotypes evolve and in what direction, depends not only on their genetic basis--both the number and effect size of causal loci--and the intensity and nature of selection acting upon them, but also on their associations with other traits. Because of genetic covariance, developmental and phylogenetic constraints, and/or correlated selection pressures (Agrawal and Stinchombe 2009), phenotypic traits often do not evolve independently from one another. Among these causal mechanisms, strong genetic covariance arises either because different traits have a shared genetic basis (pleiotropy) or because they are based on genes that are physically adjacent and therefore often co-inherited (via linkage). Strong pleiotropy is often proposed to constrain phenotypic evolution by preventing correlated traits from moving efficiently towards their own (different) fitness optima (antagonistic pleiotropy). However, such shared genetic control may also promote phenotypic change if covariation is aligned in the direction of selection (adaptive pleiotropy) (Agrawal and Stinchombe 2009; Wagner and Zhang 2011; Smith 2016). Nonetheless, despite some detailed studies (e.g. Ettensohn 2013; Shrestha et al. 2014; Manceau et al. 2011; Xu and Schluter 2015), the genetic architecture of many ecologically important traits remains unclear, including the prevalence of strong genetic associations that could shape the course of phenotypic evolution.

How shared architecture influences phenotypic change is especially relevant for suites of traits that are functionally integrated (Armbruster et al. 2014) -- such as the angiosperm flower (Armbruster et al. 2009) -- because the magnitude and direction of

pleiotropy will directly shape if and how these co-varying traits respond to selection. Further, because pleiotropy can constrain or favor particular developmental trajectories, it is often proposed to be a main driver of convergent transitions of integrated traits in different lineages (Preston et al. 2011; Smith 2016). The flower is an especially promising model for assessing the role of pleiotropy in shaping phenotypic evolution. Because flowers mediate fitness through their critical reproductive role, their constituent traits (i.e. reproductive structures, perianth, and other attraction/reward features) are often highly functionally integrated (Conner 2002; Armbruster et al. 2009). Moreover, repeated transitions of phenotypically similar or convergent suites of floral traits have been identified both within and across groups (Fenster et al. 2004; Goodwillie et al. 2010; Wessinger et al. 2016). For example, multiple parallel shifts from bee-pollination to hummingbird-pollination are associated with parallel transitions to flowers with red petals, large amounts of dilute nectar, and narrow corolla tubes within *Penstemon* (Wessinger et al. 2016); similarly, the evolution of the 'selfing syndrome' (i.e. reduced overall size, herkogamy, and floral rewards) often accompanies transitions from outcrossing to predominantly selfing mating systems, and has been documented in multiple lineages (Stebbins 1974; Goodwillie et al. 2010). Such patterns provide an opportunity to assess the relative frequency of adaptive vs. antagonistic pleiotropy in shaping these repeated trait combinations, within a comparative phylogenetic context.

In addition to these ecological and evolutionary features, the known genetic and molecular bases of floral development (Rijpkema et al. 2006; Smaczniak et al. 2012) themselves suggest that pleiotropy might be a key component shaping floral phenotypic change, as well as provide a functionally-informed framework for identifying how

changes in these mechanisms can contribute to the diversification of floral traits. Under the ABC(DE) model of floral development, the combinatorial action of different gene products -- primarily different MADS-box transcription factors -- control transitions to flowering and the specification of floral organ identities and organ maturation, by promoting or repressing different downstream targets (reviewed in O'Maoileidigh et al. 2014; Bartlett 2017). This combinatorial function, and the ability to regulate shared or partially shared downstream targets, provides a potential mechanistic explanation for strong pleiotropy among floral traits. Moreover, several key regulators of floral development also function during fruit and seed production (Smaczniak et al. 2012; O'Maoileidigh et al. 2014); such correlated effects on fertility traits are another potential way that pleiotropy could shape floral phenotypic evolution.

Several empirical approaches have been taken to assess the genetic architecture underlying floral trait specification and evolution, and to evaluate the strength and direction of pleiotropy. Classical quantitative genetic analyses have revealed varying degrees of genetic covariance among floral traits (Gottlieb 1984; Conner et al. 2014), while numerous QTL (quantitative trait locus) mapping studies have found that loci for at least some different floral traits appear to co-localize to the same genomic region(s) (reviewed in Smith 2016). Interestingly, such studies have identified more putative cases of adaptive pleiotropy (e.g. QTL affect more than one trait in the direction of parental trait values) than antagonistic, suggesting that adaptive pleiotropy may be a common mechanism contributing to rapid floral evolution. Because QTL generally span a genomic region that contains more than one gene, such QTL co-localization is consistent with, but not definitive evidence of, a role of pleiotropy in shaping floral trait co-variation (e.g. see

Hermann et al. 2013). Nonetheless, identifying strong trait correlations and/or QTL co-localization represents a critical step in assessing how pervasive pleiotropy could be in shaping floral trait evolution.

In this study, we examined phenotypic (co)variation among, and the genetic architecture underlying, floral and other reproductive traits within a segregating hybrid population derived from two *Jaltomata* (Solanaceae) species with divergent floral traits (**Figure 1**). Despite only having diversified with the last 5 million years (Sarkinen et al. 2013; Wu et al. 2018), species of *Jaltomata* are highly phenotypically diverse, including extensive variation in the size, shape, and color of floral traits that is absent among their close relatives within *Solanum* and *Capsicum*. Indeed, phylogenetic analyses suggest numerous transitions in floral traits within the genus, including several instances of convergent evolution (Miller et al. 2011; Wu et al. 2018). Importantly, many of these transitions appear to involve parallel changes in several different traits within a lineage (e.g. from flat corollas with small amounts of lightly colored nectar to highly fused corollas with large amounts of darkly colored nectar), suggesting either a shared genetic basis and/or correlated selection (perhaps pollinator-mediated selection, Fenster et al. 2004) influences these trait associations.

Here, we identified QTL contributing to floral and other reproductive trait variation within a recombinant population to: 1) examine the genetic architecture underlying reproductive trait divergence; 2) assess the role of genetic linkage and/or pleiotropy (via strong trait correlations and overlapping QTL) in floral trait (co)variation; and 3) assess evidence for a shared genetic basis between different classes of floral trait and other reproductive (specifically fertility) traits. We found evidence for a relatively

simple genetic basis underlying most of the examined traits, as well as positive correlations and significant QTL co-localization among traits within each of three trait classes (floral morphology, floral color, and fertility). Together, these features might facilitate rapid changes in these traits. In comparison, we found few associations between traits from different classes, and therefore little evidence for antagonistic pleiotropy among these classes. One striking exception was an association between flower size and nectar traits that acts in the direction exhibited by multiple species in the genus, suggesting that this could instead be an instance of adaptive pleiotropy.

## MATERIALS AND METHODS

***Study system:*** *Jaltomata* (Schlechtendal; Solanaceae) is the sister genus to the large and economically important *Solanum* (Olmstead et al. 2008; Sarkinen et al. 2013; Wu et al. 2019), and includes approximately 60-80 species distributed from the Southwestern United States to the Andean region of South America, in addition to several species endemic to the Greater Antilles and the Galapagos Islands (Miller et al. 2011; Mione et al. 2015). Species are highly phenotypically diverse and live in a variety of habitats (e.g. tropical rainforests, rocky foothills, and *lomas* formations), despite their recent divergence (<5MYA, Sarkinen et al. 2013).

Here, we focused on a closely related species pair, *J. sinuosa* and *J. umbellata*, that differ in a suite of floral traits that is representative of major floral suites found in other species throughout the genus (**Figure 1**; **Table S1**). *Jaltomata sinuosa* has large rotate flowers with purple petals and a small amount of concentrated nectar (consistent with bee pollination, Fenster et al. 2004), while *J. umbellata* has small short-tubular

flowers with white petals and a large amount of dilute, but dark red, nectar that is visible through the corolla tube (consistent with hummingbird pollination, Fenster et al. 2004; Kostyun and Moyle 2017; Mione et al. 2017). *Jaltomata sinuosa* is distributed along the Andes in South America from Venezuela to Bolivia, while *J. umbellata* is restricted to lomas formations along the Peruvian coast. Both species are self-compatible (Kostyun and Moyle 2017; J.L. Kostyun and T. Mione, unpub.) and shrubby, but differ in leaf traits such as overall size and shape, and type of trichomes. This species pair also has several incomplete, intrinsic postzygotic reproductive barriers, including quantitatively reduced fruit set and hybrid seed viability (Kostyun and Moyle 2017).

***Generation of $BC_1$ population and plant cultivation:*** We developed a segregating hybrid population by crossing *J. sinuosa* and *J. umbellata*. Viable F1 individuals in both directions of the cross produce flowers that are phenotypically intermediate between the parental genotypes (**Figure 1**), and retain reduced but sufficient levels of fertility when back-crossed to parents (Kostyun and Moyle 2017). Because we were especially interested in the genetic basis of red nectar and a fused corolla tube (exhibited by *J. umbellata* and F1s but not *J. sinuosa*), we generated the mapping population by backcrossing a single *J. sinuosa* x *J. umbellata* F1 (as the ovule parent) to the original parental *J. sinuosa* individual (as the pollen parent). BC1 individuals were germinated in a growth chamber, and then moved to the Indiana University greenhouse and grown under the same conditions as the parental and F1 individuals (16 hour light cycle, watered twice daily, and fertilized weekly).

***Trait measurements:*** We measured 25 floral and other reproductive traits within our mapping population, F1, and parental genotypes (**Table 1; Table S2; Figure S1**).

Floral morphological traits were measured with hand-held calipers, and nectar volume per flower was measured to the nearest 1 μL using a pipette. To reduce the potential effect of daily environmental variation, nectar volume was always measured in the early afternoon following watering.

Petal and nectar color were quantified using digital photography (Kendal et al. 2013; Garcia et al. 2014): dissected petals and nectar drops were photographed on a standard background along with white and black color standards. Light conditions were standardized for all images using RAW Therapee (RAW Therapee Development Team 2012), and color space attributes were measured in ImageJ (Schneider et al. 2012). Because RGB color attributes are device-dependent (i.e. they can vary depending upon the specific camera used), color values were also converted into device-independent L*a*b color attributes, using the ImageJ Color Space Converter plugin (Schwartzwald 2012). For both petal and nectar color, this approach produced eight interrelated color attributes: Intensity, Red, Green, Blue, Composite RGB, Lightness (L), 'a' color (ranges from green to magenta), and 'b' color (ranges from cyan to yellow). Broadly, Intensity, Red, Green, Blue, and Lightness convey information about color brightness, while Composite RGB, 'a' color, and 'b' color convey information about hue.

We also measured nine fertility traits (**Table 1**) to assess the potential genetic overlap between floral and other reproductive traits, as well as to examine the genetic architecture underlying intrinsic postzygotic barriers between this species pair. Fruit and seed related traits were measured on 2-6 crossed fruit per individual (depending on fruit set). For F1 and BC1 individuals, crossed fruit were produced using pollen from the *J. sinuosa* parental individual. To determine seed germination rates (following Farooq et al.

2005), we soaked 10 seeds per individual in 50% bleach for 30 minutes (to soften the seed coat), rinsed thoroughly, and placed on moist paper within plastic germination boxes. A week after sowing, seed coats were nicked slightly and seeds were given a drop of 10 mM giberellic acid (Sigma) to break dormancy. We then scored germination every 2 weeks for 4 months. Pollen viability was estimated from three different flowers per individual, using established methods (Jewell et al. 2012): Briefly, for each sample all undehisced anthers from a flower were collected into an eppendorf tube containing aniline blue histochemical stain, gently ground with a pestle to release pollen, and viable pollen grains were counted under an EVOS FL Digital Inverted Fluorescence Microscope (Fisher Scientific). From these data, we also calculated the proportion of viable pollen as number of viable pollen grains/total pollen grains in the sample.

***Statistical analyses on phenotypic data***: Following Shapiro-Wilk tests to assess normality assumptions, we transformed traits that showed a skewed distribution and/or significantly non-normal residuals. In particular, we arcsine transformed proportional traits (proportion of corolla fusion, fruit set, and proportion of viable pollen), and log-transformed inflorescence size, corolla fusion, petal length, style length, herkogamy, nectar volume, all color attributes, and remaining fertility traits. Significant differences between parental species for all traits were assessed by t-tests (**Table 1**). Distribution plots for all traits are provided in Supplementary Materials (**Figures S2-S6**), while illustrative plots for 15 focal traits are provided in the main text (**Figure 2**). Similarly, phenotypic correlations within the BC1 population were examined among all traits (**Table S3**), while relationships among a subset of focal traits are presented in the main text (**Figure 3**). Given significant correlations among many of the floral morphological

traits and among color attributes (**Table S3**), we also used principle component analyses (PCAs) to create separate composite metrics (principle components (PCs)) for three groups of traits (i.e. Morph PC1-PC3; Nectar Color PC1-3; Petal Color PC1-PC3; **Table S4**) as additional measures of floral variation. Trait correlations, including PCs, are provided in **Table S5**, and distribution plots are provided in **Figures S3-S5**.

***Genotyping and linkage map construction:*** Genomic DNA was extracted from young leaf tissue from the 2 parental individuals, 13 F1s (including the F1 parent used to generate the population), and 269 BC1s, using the Qiagen DNeasy Plant Mini Kit. DNA quantity and quality were confirmed via Nanodrop (Fisher Scientific) and gel electrophoresis with λ DNA-HindIII Digest marker (New England BioLabs). Samples were then sent to Novogene Corporation (Beijing) for genotyping-by-sequencing (GBS). GBS libraries were prepared using optimized restriction enzymes (MseI and HaeIII), and following insert size selection, sequenced on an Illumina Hi-Seq to generate 150bp paired end reads. Raw reads were trimmed and filtered using Trimmomatic (Bolger et al. 2014), and read quality was checked pre- and post-trimming using fastqc (Andrews 2010). To identify SNPs, cleaned reads were mapped to the domesticated tomato genome (Tomato Genome Consortium 2012) using the mem function in BWA (Li 2013). Alignment files were then input into the STACKS refmap pipeline (Catchen et al. 2013) to determine genotypes. Reads and genotype data are available in NCBI SRA XXXXXX.

To construct the linkage map, we first removed markers that were genotyped in less than 35% of individuals, or showed significant segregation distortion (i.e. alleles at >80% or <20% frequency). The linkage map was constructed using the MST and Kosambi algorithms, implemented in the R package ASMap (Taylor and Butler 2017).

To alleviate map expansion issues, we removed markers which consistently differed from neighboring markers in terms of genotype assignment, indicating a high likelihood of genotyping error. The linkage map was then finalized using the ripple function in R package R/qtl (Broman et al. 2003).

***Identifying QTL:*** We implemented Haley-Knott regression in R/qtl to identify QTL contributing to each trait. To account for potential environmental contributions to trait variation, we included date of measurement (Month) and location within the greenhouse (Bench) as covariates in our QTL scans. Putative QTL were first identified using the scanone function, followed by permutations for genome-wide LOD significance thresholds. Two dimensional scans (scantwo function) were used in the stepwise qtl function to fit multiple QTL models. These models were used to identify significant QTL, their 1.5 LOD confidence intervals, their effect sizes (i.e. difference in phenotype mean between homozygotes and heterozygotes), and the total amount of phenotypic variance explained by each QTL, as well as interactions among QTL, and potential contributions of covariates. QTL were considered to be co-localized if their 1.5 LOD intervals overlapped. Significant co-localization was assessed by comparing overlap among identified QTL to overlap from 10000 randomly generated distributions, for traits within each category (morphological, color/physiological, or fertility), and between each trait category. Briefly, a custom Python script was used to generate random distributions of QTL (by randomly re-distributing the identified QTL among the 12 linkage groups), and the observed frequency of co-localization in each was recorded for each randomization to generated count distributions, in R. All code used to generate the linkage map, identify QTL, and assess QTL co-location, is available on GitHub

(https://github.com/gibsonMatt/jaltomataQTL).

## RESULTS

### *Segregation patterns suggest additive alleles underlie most traits*

Most traits were significantly different between the two parental species (**Table 1**). F1 means were intermediate for most traits as well, except that petals were generally brighter (more white) than either parent (**Figures S5+S7**). Other than fruit set and seed germination rates, all traits were unimodally distributed within the BC1s; phenotypic values were intermediate between F1s and the recurrent parent (*J. sinuosa*) for many of these traits, consistent with additive effects (**Figure 2; Figures S2-S6**). Several traits (7 of 25) showed transgressive segregation within the BC1s, including some floral morphological traits, nectar volume and color, and seed viability and germination rates (**Table S2; Figures S2-S6**).

### *Significant correlations observed within – but generally not between – floral morphology, floral color, and fertility trait categories*

Within the BC1s, most trait combinations were not strongly associated. Nonetheless, several correlations remained significant following multiple testing (Bonferroni) correction (**Table S3**), primarily associations that are expected biologically, including allometric relationships among floral organs and positive associations among related fertility traits. For instance, corolla diameter was significantly positively associated with most other morphological traits, suggesting shared genetic control of overall floral size (**Figure 3**), while corolla diameter was also significantly negatively

correlated with proportion of corolla fusion (i.e. shorter corolla tubes had wider limbs and longer tubes had narrower limbs, r = -0.348, $p = 8.68e^{-8}$). These relationships were recovered with PCA on morphology traits, in which PC1-PC3 explained 76% of the variance among BC1s (**Table S4**). Based on trait loadings, PC1 corresponds to floral width vs. depth, PC2 to overall floral size, and PC3 to relative reproductive organ dimensions. Similarly, related fertility traits also remained strongly correlated, such as fruit mass with seed set, and number of viable pollen grains with proportion of viable pollen (**Table S3**). Finally, color attributes within each of nectar color and petal color were strongly correlated with one another, but these attributes were not associated between nectar and petals (**Table S3**). From PCAs on nectar color and petal color attributes (separately), PC1-PC3 for each explained 97% and 94% of the variance among BC1s, respectively (**Table S4**).

In contrast, there were relatively few significant correlations among different trait categories. Notable exceptions, however, included a positive relationship between floral size and nectar volume as well as floral size and certain aspects of nectar color (**Figure 3; Table S3**). There were also significant positive correlations between pollen viability and each of several components of flower size (as well as Morph PC2 or "size") (**Tables S3+S5**). This latter relationship seems to be explained by anther size: across 15 *Jaltomata* species, mean viable pollen count is significantly associated with anther size prior to dehiscence ($F = 15.56$, $p = 0.0017$) (J.L. Kostyun, unpub.).

***Linkage map construction recovered 12 linkage groups***

Mapping high quality reads to the tomato genome identified 25,136 SNPs that

differentiated the two parental species. Following all subsequent filtering (removing markers genotyped in less than 35% of individuals, with high segregation distortion or non-Mendelian inheritance, or with high likelihood of genotyping errors), we retained 520 high quality markers. Linkage map construction recovered 12 linkage groups (LGs), which correspond to the number of chromosomes in the parental species (Mione et al. 1993; Chiarini et al. 2017). Based on orthology with tomato, we were able to confidently assign 5 of these LGs to chromosomes (**Figure 4**). Total map length was 1593.71 cM (65.17 cM – 324.48 cM per chromosome/LG), with an average of 2.92 cM between markers (**Figure 4**).

***Few moderate-effect QTL underlie most traits, with little QTL co-localization between trait categories***

We identified a total of 63 QTL for our 25 traits (with 4 additional loci for PC traits). Most traits had 2-4 QTL, with a range of 0-6 QTL (**Table 2**, **Table S6**). Alleles at 55 of 67 QTL (82%) acted in the direction consistent with parental values (i.e. the allele from paternal donor *J. umbellata* moved the phenotype of BC1s closer to its species mean) (**Table 2**), and the amount of phenotypic variation explained per QTL ranged from 2-28%. The latter range suggests that we had reasonable power to identify QTL with even relatively small effects--explaining as little as 2% of the variance. Consistent with observed trait segregation patterns, significant interactions among QTL within individual traits were identified in few cases: for ovary diameter and certain nectar color attributes (**Table 2**, **Table S6**).

Although every linkage group had at least one QTL, QTL were not distributed

uniformly across the genome, with notable clusters on LG1 and LG9 (**Figure 4, Table 2**). We also identified several instances of QTL co-localization within trait categories, especially for morphology and fertility traits, which each had significantly more cases of co-localization (1.5 LOD overlap) than expected by chance (133 observed vs. upper bound of 115 expected overlaps, $p = 7.5e^{-4}$; 8 observed vs. upper bound of 4 expected overlaps, $p = 7.0e^{-6}$, respectively) (**Table S7; Figure S8**). These co-localization instances included QTL for biologically-related traits (e.g. petal length and corolla diameter, or fruit mass and seed set; **Table S6**), for which we already observed strong correlations (**Table S3**). In some cases, co-localized QTL share the same or a very close peak marker (e.g. petal length, corolla fusion, and ovary diameter on LG12; **Table S6**) which is suggestive of potential pleiotropy, however we note that the large 1.5 LOD intervals of some QTL will increase instances of incidental co-localization events.

In contrast, co-localization between different trait categories was never greater than expected by chance, with co-localization between morphology and color traits actually significantly less than expected ($p = 0.016$) (**Table S7; Figure S8**). This is consistent with mostly incidental occurrences of overlap between QTL for traits in different categories. Nonetheless, we did detect co-localized QTL at the same or very close peak markers for, for example, nectar color (RGB) and volume on LG3 (**Figure 4; Table S6**) and for nectar color (a), corolla fusion, and corolla depth on LG7, (**Table S6**), which provide intriguing cases of potential adaptive pleiotropy (i.e. alleles at QTL that simultaneously act to increase floral size, nectar darkness, and/or nectar volume).

## DISCUSSION

Genetic correlations among different components of the phenotype, especially resulting from pleiotropy, can constrain or facilitate trait evolution (Agrawal and Stinchcombe 2009). Pleiotropy could have particularly strong effects on the evolution of traits that are functionally integrated, such as those comprising the flower (Armbruster et al. 2009; Smith 2016). To better understand the genetic architecture underlying floral trait evolution within florally diverse *Jaltomata*, including whether pleiotropy might have shaped observed variation, we examined patterns of genetic segregation and genetic architecture for 25 floral and fertility traits in a hybrid (BC1) population between species with highly divergent floral traits. We found that most of our examined traits have a relatively simple genetic basis, with few to moderate QTL with largely additive effects. We also identified strong correlations and significant QTL overlap within trait categories, but few associations across different types of traits. The exceptions however, between certain aspects of floral morphology and nectar traits, are consistent with existing trait associations that are observed across the genus, suggesting that these could be examples of adaptive pleiotropy. Overall, our data suggest that the rapid floral trait evolution observed in this group could have been facilitated by a relatively simple genetic basis for individual floral traits, and a general absence of antagonistic pleiotropy among different types of reproductive traits, especially morphology and color.

***Few genetic changes could underlie floral trait shifts***

The relatively simple genetic architecture that we detect for most of our floral traits might be one mechanism that has permitted rapid floral evolution within the genus. Indeed, our inference that few QTL controlling corolla traits agrees with comparative

development data from these species (Kostyun et al. 2017) in which we observe that relatively simple heterochronic changes in corolla trait growth rates distinguish these rotate vs. tubular corolla forms. Interestingly, our findings are also consistent with previous studies of floral trait genetics between closely related species (Smith 2016). For instance, one or few QTL have been found for species differences in nectar volume in several other systems (e.g. Bradshaw et al. 1998; Stuurman et al. 2004; Wessinger et al. 2014; but see Nakazato et al. 2013), similar to our inference of a single QTL for this trait. For petal and nectar color, we identified 2 and 5 QTL, respectively, each with moderate to major effects (**Table 2, Table S6**), similar to other systems that generally identify few loci of large effect for petal color (e.g. Bradshaw et al. 1998; Wessinger et al. 2014). Perhaps unlike these cases, however, it is likely that loci controlling color differences in *Jaltomata* are regulators of pigment quantity rather than presence/absence biosynthesis, because both nectar and petal color show gradation in the BC1s rather than discrete color bins. Moreover, preliminary data from a VIGS (virus-induced gene silencing) pilot study in *J. sinuosa* indicate that the purple petal pigment is an anthocyanin (J.L. Kostyun and J.C. Preston, unpub.), whereas for nectar color, preliminary data suggest that an indole-flavin contributes to red pigment in *J. umbellata* (J.L. Kostyun and D. Haak, unpub.), consistent with our inference that color variation is unassociated between these different floral components.

In addition to relatively few contributing loci, many of the examined traits also appear to be underpinned by additive effects (**Table 1; Figure 3; Figures S2-6**), while epistatic effects were comparatively rare. Both are factors that might also facilitate more rapid responses to selection. Other studies have similarly found that floral size traits are

often additive (Gottlieb 1984). Although several floral traits showed transgressive segregation within our BC1s, which could indicate epistatic interactions, similar patterns can result from unique combinations of additive alleles that have opposite effects in the parental species (e.g. deVicente and Tanksley 1993) and we identified individual QTL with these opposing effects for many of these traits. In comparison, significant interaction effects among morphological QTL were detected for ovary diameter only (**Table 2**), consistent with a general lack of epistatic interactions for this class of traits.

The notable exceptions to additivity involved many of the fertility traits (as well as some components of color, see below). BC1 individuals tended to have lower seed set and poorer quality seeds (decreased viability and response to germination-inducing stimuli), and the recombinant BC population contained a subset of highly sterile individuals. The segregation of recombinant individuals with reduced viability and fertility often occurs in hybrids (Baack et al. 2015), including in hybrids from additional *Jaltomata* species pairs (Kostyun and Moyle 2017). Such patterns are typically due to deleterious epistatic interactions between loci that have diverged between the two parental lineages, as has been shown in close relatives including tomatoes (Moyle and Nakazato 2008; Sherman et al. 2014). These observations in *Jaltomata* are similarly consistent with a specific role for epistasis among incompatible alleles in the expression of postzygotic reproductive isolation.

***Reduced constraints may also have facilitated rapid floral trait evolution***

Because rapid floral evolution may occur either through a lack of antagonistic pleiotropy or through adaptive pleiotropy, we assessed evidence for these potential

439 mechanisms within *Jaltomata*. Within trait categories, we detected positive but modest
440 associations between several floral size traits, and among biologically related fertility
441 traits (e.g. fruit size and seed set) (**Figure 3; Table S3**), as well as significant co-
442 localization of QTL for these groups of traits (**Table S7**). Morphological associations in
443 particular suggest that shared growth regulators (e.g. Sicard and Lenhard 2011; Brock et
444 al. 2012) contribute to - but do not completely determine - observed variation in floral
445 organ sizes. In contrast, we detected fewer instances of strong trait correlations and QTL
446 co-localization between different trait categories (**Table S3**, **Table S7**). This general lack
447 of antagonistic pleiotropy among different classes of floral and fertility traits may have
448 facilitated rapid floral evolution in this system by minimizing constraints on the available
449 combinations of floral traits. Despite this general pattern, we did identify several
450 instances of QTL co-localization that might represent adaptive pleiotropy. Most notably,
451 larger flowers generally produced darker (more red) nectar as well as a greater volume of
452 nectar, as reflected in co-localization of QTL underlying aspects of floral morphology
453 and both nectar volume and color (**Table 2; Figure 4; Table S6**). Interestingly, this trait
454 combination (large flowers with copious dark nectar) is actually not exhibited by either
455 parental species used in this experiment (**Figure 1; Table 1**); however, it is found in
456 numerous other *Jaltomata* species (see below; Miller et al. 2011; Kostyun and Moyle
457 2017) and is consistent with recognized pollination syndromes (e.g. Fenster et al. 2004).
458
459 ***Ecological context for rapid floral change in* Jaltomata**
460 Overall, our findings suggest potential mechanistic explanations for the evolution
461 of remarkable floral trait diversity among *Jaltomata* species within the last 5 million

462 years (Sarkinen et al. 2013). Traits with a relatively simple genetic basis that are
463 uncoupled from other floral and fertility traits have fewer mechanistic constraints, and
464 therefore can more rapidly respond to selective opportunities as they arise. Although we
465 have not yet directly assessed the role of selection in shaping floral differences among
466 species, several features of *Jaltomata* floral biology are consistent with pollinator-
467 mediated selection on floral traits (van der Niet and Johnson 2012), likely in conjunction
468 with mating-system related changes (Goodwillie et al. 2010). First, floral trait variation
469 within *Jaltomata* shows clear hallmarks of selection imposed by pollinator
470 differentiation. Nearly all species in the earliest diverging *Jaltomata* lineage have
471 relatively small, ancestrally rotate flowers with small amounts of lightly colored nectar,
472 and hymenopterans have been observed visiting several of these species (T. Mione, pers.
473 comm.). In contrast, many species in the South American derived clade—including *J.*
474 *umbellata* examined here--have attractive features associated with vertebrate pollination
475 (Fenster et al. 2004). Several of these are visited by hummingbirds (T. Mione, per.
476 comm.), notably those with larger flowers with a highly fused corolla (either campanulate
477 or tubular) and copious amounts of darkly colored nectar; intriguingly, this repeated
478 natural trait covariation is consistent with the genetic association between floral size and
479 nectar traits we identified here.

480 These features indicate that pollinators are a likely source of selection for floral
481 differentiation among species within *Jaltomata*, but they do not necessarily explain why
482 *Jaltomata* as a genus has been uniquely responsive to this pollinator variation, especially
483 in comparison to its most close relatives. Species from both *Solanum* and *Capsicum* are
484 found within the same geographical regions as *Jaltomata*, and are therefore exposed to

485 the same pollinator variation, but are nonetheless almost uniformly rotate and bee-
486 pollinated (Knapp 2010). Interestingly, one important difference between *Jaltomata* and
487 these two genera is in their predominant mating system. Self-incompatibility is the
488 ancestral state in the Solanaceae (Steinbachs and Holsinger 2002) and is broadly
489 persistent in both *Solanum* and *Capsicum* (Goldberg et al. 2010). In contrast, all
490 examined *Jaltomata* species are self-compatible (Mione 1992; J.L. Kostyun and T.
491 Mione, unpub.), indicating that gametophytic self-incompatibility was lost early in the
492 evolution of this clade. Moreover, the presence of delayed selfing and strong herkogamy
493 in many species (e.g. Mione et al. 2015; Mione et al. *in review*), in addition to field
494 observations of pollinators (above; T. Mione, pers. comm.), indicate that species most
495 likely employ a mixed mating strategy in their native ranges. The absence of genetically-
496 determined self-incompatibility and the predominance of mixed mating strategies might
497 have uniquely facilitated the evolution of new floral trait variation in *Jaltomata*,
498 compared to either *Capsicum* or *Solanum*. Mixed mating strategies are generally
499 observed to maintain the largest amount of floral trait variation, compared to predominant
500 selfing or enforced outcrossing (Goodwillie et al. 2005; Rosas-Guerrero et al. 2014). In
501 addition, they have been predicted to facilitate pollinator shifts--especially to pollinators
502 that might be more efficient but potentially unreliable (such as hummingbirds)—because
503 they allow reproductive assurance (via selfing, when pollinators are limited) and increase
504 the expression of new floral trait variation controlled by recessive alleles (Goodwillie et
505 al. 2005; Brys et al. 2013; Wessinger and Kelly 2018). Notably, our data indicate that
506 dark/red colored nectar is at least partially recessive (**Figure 2**), and that red petal
507 pigmentation is completely recessive (**Figure S7**), consistent with this novel variation

508 being based on new recessive alleles.

509

510 **CONCLUSIONS**

511 Genetic correlations among floral traits, especially those due to pleiotropic
512 effects, likely shape permitted trajectories of floral evolution. To assess how such genetic
513 associations might have contributed to observed patterns of floral diversity in *Jaltomata*,
514 we examined segregation patterns and genetic architecture of 25 floral and fertility traits
515 in a hybrid (BC1) population generated from parents with divergent floral traits. Our data
516 are consistent with several mechanisms that could have allowed rapid floral trait
517 evolution in this system: a largely simple genetic basis underlying variation in most of
518 our floral traits, a general absence of antagonistic pleiotropy constraining floral evolution,
519 and a potential instance of adaptive pleiotropy governing floral size and nectar traits. This
520 genetic architecture, in combination with pollinator-mediated selection on a background
521 of self-compatible mixed mating, might have uniquely positioned this genus for the rapid
522 floral diversification now evident within *Jaltomata*.

523

524 **ACKNOWLEDGEMENTS**

525 We thank the IU greenhouse staff for plant care, CJ Jewell and David Haak for
526 logistical support, undergraduate research assistants (especially Meret Thomas-Huebner,
527 Devki Shukla, and Shachia Jackson) for assistance with data collection, and Tim Leslie
528 for assistance with simulations. This work was supported by the IU Biology Department,
529 National Science Foundation Award (NSF DEB 1136707) to LCM, and National Science
530 Foundation Graduate Research Fellowship Program (NSF DEB 1342962) and Doctoral

Dissertation Improvement Grant (NSF DEB 1601078) to JLK.

## AUTHOR CONTRIBUTIONS

JLK and LCM designed the experiment, JLK generated experimental materials, JLK and CMK collected phenotypic data, JLK and MJSG analyzed the data, and JLK and LCM wrote the paper with input from CMK and MJSG.

## REFERENCES

Agrawal, A. F., and J. R. Stinchcombe. 2009. How much do genetic covariances alter the rate of adaptation? *Proc R Soc Lond Biol* **276**:1183-1191.

Andrews, S. 2010. FastQC: a quality control tool for high throughput sequence data. Available online at: http://www.bioinformatics.babraham.ac.uk/projects/fastqc

Armbruster, W. S., T. F. Hansen, C. Pelabon, R. Perez-Barrales, and J. Maad. 2009. The adaptive accuracy of flowers: measurement and microevolutionary patterns. *Ann Bot* **103**:1529-1545.

Armbruster, W. S., C. Pelabon, G. H. Bolstad, and T. F. Hansen. 2014. Integrated phenotypes: understanding trait covariation in plants and animals. *Proc R Soc Lond Biol* **369**.

Baack, E., M. C. Melo, L. H. Rieseberg, and D. Ortiz-Barrientos. 2015. The origins of reproductive isolation in plants. *New Phytol* **207**:968-984.

Bartlett, M. E. 2017. Changing MADS-Box Transcription Factor Protein–Protein Interactions as a Mechanism for Generating Floral Morphological Diversity. *Integrative and Comparative Biology* **57**:1312-1321.

554 Bradshaw, H. D., K. G. Otto, B. E. Frewen, J. K. McKay, and D. W. Schemske. 1998.
555 Quantitative trait loci affecting differences in floral morphology between two
556 species of monkeyflower (*Mimulus*). *Genetics* **149**:367-382.
557 Brock, M. T., P. X. Kover, and C. Weinig. 2012. Natural variation in GA1 associates
558 with floral morphology in *Arabidopsis thaliana*. *New Phytol* **195**:58-70.
559 Broman, K. W., H. Wu, S. Sen, and G. A. Churchill. 2003. R/qtl: QTL mapping in
560 experimental crosses. *Bioinformatics* 19:889-890.
561 Brys, R., B. Geens, T. Beeckman, and H. Jacquemyn. 2013. Differences in dichogamy
562 and herkogamy contribute to higher selfing in contrasting environments in the
563 annual *Blackstonia perfoliata* (Gentianaceae). *Ann Bot* **111**:651-661.
564 Bolger, A. M., M. Lohse, and B. Usadel. 2014. Trimmomatic: A flexible trimmer for
565 Illumina Sequence Data. *Bioinformatics*, btu170.
566 Catchen, J., P. A. Hohenlohe, S. Bassham, A. Amores, and W. A. Cresko. 2013. Stacks:
567 an analysis tool set for population genomics. *Mol Ecol* 22: 3124-3140.
568 Chiarini, F. E., D. Lipari, G. E. Barboza, and S. Knapp. 2017. In: IAPT/IOPB
569 chromosome data 25. K. Marhold and J. Kuccera (eds). *Taxon* 66: 1246–1252.
570 Conner, J. K. 2002. Genetic mechanisms of floral trait correlations in a natural
571 population. *Nature* **420**:407-410.
572 Conner, J. K., I. A. Cooper, R. J. La Rosa, S. G. Perez, and A. M. Royer. 2014. Patterns
573 of phenotypic correlations among morphological traits across plants and animals.
574 *Phil. Trans. R. Soc. B* **369**.
575 deVicente, M. C., and S. D. Tanksley. 1993. QTL analysis of transgressive segregation in
576 an interspecific tomato cross. *Genetics* **134**:585-596.

577 Ettensohn, C. A. 2013. Encoding anatomy: Developmental gene regulatory networks and
578 morphogenesis. *Genesis* **51**:383-409.
579 Farooq, M., S. M. A. Basra, N. Ahmad, and K. Hafeez. 2005. Thermal hardening: A new
580 seed vigor enhancement tool in rice. *J Integr Plant Biol* **47**:187-193.
581 Fenster, C. B., W. S. Armbruster, P. Wilson, M. R. Dudash, and J. D. Thomson. 2004.
582 Pollination syndromes and floral specialization. *Annu Rev Ecol Evol Syst* **35**:375-
583 403.
584 Garcia, J. E., A. D. Greentree, M. Shrestha, A. Dorin, and A. G. Dyer. 2014. Flower
585 Colours through the Lens: Quantitative Measurement with Visible and Ultraviolet
586 Digital Photography. *Plos One* **9**.
587 Goldberg, E. E., J. R. Kohn, R. Lande, K. A. Robertson, S. A. Smith, and B. Igic. 2010.
588 Species selection maintains self-Incompatibility. *Science* **330**:493-495.
589 Goodwillie, C., S. Kalisz, and C. G. Eckert. 2005. The evolutionary enigma of mixed
590 mating systems in plants: Occurrence, theoretical explanations, and empirical
591 evidence. *Annu Rev Ecol Evol Syst* **36**:47-79.
592 Goodwillie, C., R. D. Sargent, C. G. Eckert, E. Elle, M. A. Geber, M. O. Johnston, S.
593 Kalisz, D. A. Moeller, R. H. Ree, M. Vallejo-Marin, and A. A. Winn. 2010.
594 Correlated evolution of mating system and floral display traits in flowering plants
595 and its implications for the distribution of mating system variation. *New Phytol*
596 **185**:311-321.
597 Gottlieb, L. D. 1984. Genetics and morphological evolution in plants. *Am Nat* **123**:681-
598 709.
599 Hermann, K., U. Klahre, M. Moser, H. Sheehan, T. Mandel, and C. Kuhlemeier. 2013.

Tight Genetic Linkage of Prezygotic Barrier Loci Creates a Multifunctional Speciation Island in *Petunia*. *Current Biology* **23**:873-877.

Jewell, C., A. D. Papineau, R. Freyre, and L. C. Moyle. 2012. Patterns of reproductive isolation in *Nolana* (chilean bellflower). *Evolution* **66**:2628-2636.

Kendal, D., C. E. Hauser, G. E. Garrard, S. Jellinek, K. M. Giljohann, and J. L. Moore. 2013. Quantifying Plant Colour and Colour Difference as Perceived by Humans Using Digital Images. *Plos One* **8**.

Knapp. S. 2010. On 'various contrivances': pollination, phylogeny and flower form in the Solanaceae. *Phil Trans R Soc B* 365:449-460.

Kostyun, J. L. and L. C. Moyle. 2017. Multiple strong postmating and intrinsic postzygotic reproductive barriers isolate florally diverse species of *Jaltomata* (Solanaceae). *Evolution* **71**:1556-1571.

Kostyun, J. L., J. C. Preston, and L. C. Moyle. 2017. Heterochronic developmental shifts underlie floral diversity within *Jaltomata* (Solanaceae). *EvoDevo* 8(1): 17.

Li, H. 2013. Aligning sequence reads, clone sequences and assembly contigs with BWA-MEM. arXiv:1303.3997v1 [q-bio.GN].

Manceau, M., V. S. Domingues, R. Mallarino, and H. E. Hoekstra. 2011. The Developmental Role of Agouti in Color Pattern Evolution. *Science* **331**:1062-1065.

Miller, R. J., T. Mione, H. L. Phan, and R. G. Olmstead. 2011. Color by Numbers: Nuclear Gene Phylogeny of *Jaltomata* (Solanaceae), Sister Genus to *Solanum*, Supports Three Clades Differing in Fruit Color. *Syst Botany* **36**:153-162.

622 Mione, T. 1992. *The systematics and evolution of* Jaltomata *(Solanaceae)*. PhD
623 Dissertation, The University of Connecticut. Available from ProQuest
624 Dissertations & Theses Global. (303964972).
625 Mione, T., G. J. Anderson, and M. Nee. 1993. *Jaltomata* I: Circumscription, description
626 and new combinations for five South American species. *Brittonia* 45: 138-145.
627 Mione, T., S. Leiva González, and L. Yacher 2015. Two new Peruvian species of
628 *Jaltomata* (Solanaceae, Solaneae) with red floral nectar. *Brittonia* **67**:105-112.
629 Mione, T., K. C. Plourd, S. Leiva González, L. Yacher, C. T. Philbrick, and D. Blume.
630 2017. Pollination decreases longevity of the protogynous flowers of *Jaltomata*
631 *sinuosa* (Solanaceae). *J Biol Nat* **7**:123–9.
632 Mione, T., J. L. Kostyun, and S. Leiva Gonzalez. In Revision. Self-compatibility,
633 protogyny and locating the floral nectary of *Jaltomata quipuscoae* (Solanaceae).
634 Moyle, L. C., and T. Nakazato. 2008. Comparative genetics of hybrid incompatibility:
635 Sterility in two Solanum species crosses. *Genetics* **179**:1437-1453.
636 Nakazato, T., L. H. Rieseberg, and T. E. Wood. 2013. The genetic basis of speciation in
637 the Giliopsis lineage of Ipomopsis (Polemoniaceae). *Heredity* **111**:227-237.
638 Olmstead, R. G., L. Bohs, H. A. Migid, E. Santiago-Valentin, V. F. Garcia, and S. M.
639 Collier. 2008. A molecular phylogeny of the Solanaceae. *Taxon* **57**:1159-1181.
640 Preston, J. C., L. C. Hileman, and P. Cubas. 2011. Reduce, reuse, and recycle:
641 developmental evolution of trait diversification. *Am. J. Bot.* **98**:397-403.
642 RAW Therapee Team. 2012. Raw Therapee: cross-platform raw image processing
643 program. http://rawtherapee.com/.
644 Rijpkema A, T Gerats, and M. Vandenbussche. 2006. Genetics of floral development in

Petunia. Pages 237-278 *in* L. J. Soltis DE, Soltis PS & Callow JA, editor. Adv Bot Res: Incorp Adv Plant Pathol: Developmental Genetics of the Flower.

Rosas-Guerrero, V., R. Aguilar, S. Marten-Rodriguez, L. Ashworth, M. Lopezaraiza-Mikel, J. M. Bastida, and M. Quesada. 2014. A quantitative review of pollination syndromes: do floral traits predict effective pollinators? *Ecol. Lett* **17**:388-400.

Sarkinen, T., L. Bohs, R. G. Olmstead, and S. Knapp. 2013. A phylogenetic framework for evolutionary study of the nightshades (Solanaceae): a dated 1000-tip tree. *BMC Evolutionary Biology* **13**.

Schneider, C. A., W. S. Rasband, and K. W. Eliceiri. 2012. NIH Image to ImageJ: 25 years of image analysis. *Nature Methods* **9**:671-675.

Schwartzwald, D. 2012. Color Space Converter Plugin for ImageJ. https://imagej.nih.gov/ij/plugins/color-space-converter.html.

Sherman, N. A., A. Victorine, R. J. Wang, and L. C. Moyle. 2014. Interspecific Tests of Allelism Reveal the Evolutionary Timing and Pattern of Accumulation of Reproductive Isolation Mutations. *Plos Genetics* **10**.

Shrestha, R., J. Gomez-Ariza, V. Brambilla, and F. Fornara. 2014. Molecular control of seasonal flowering in rice, arabidopsis and temperate cereals. *Ann Bot* **114**:1445-1458.

Sicard, A., and M. Lenhard. 2011. The selfing syndrome: a model for studying the genetic and evolutionary basis of morphological adaptation in plants. *Ann Bot* **107**:1433-1443.

Smaczniak, C., R. G. H. Immink, G. C. Angenent, and K. Kaufmann. 2012. Developmental and evolutionary diversity of plant MADS-domain factors:

668 insights from recent studies. *Development* **139**:3081-3098.

669 Smith, S. D. 2016. Pleiotropy and the evolution of floral integration. *New Phytol* **209**:80-
670 85.

671 Stebbins, G.L. 1974. Flowering plants: evolution above the species level. Harvard
672 University Press, Cambridge, MA.

673 Steinbachs J.E., and K.E. Holsinger 2002. S-RNase-mediated gametophytic self
674 incompatibility is ancestral in eudicots. *Mol Biol Evol* **19**: 825–829.

675 Stuurman, J., M. E. Hoballah, L. Broger, J. Moore, C. Basten, and C. Kuhlemeier. 2004.
676 Dissection of floral pollination syndromes in *Petunia*. *Genetics* **168**:1585-1599.

677 Taylor, J., and D. Butler. 2017. R Package ASMap: Efficient Genetic Linkage Map
678 Construction and Diagnosis. *Journal of Statistical Software* 79:1-29.

679 Tomato Genome Consortium, The. 2012. The tomato genome sequence provides insights
680 into fleshy fruit evolution. *Nature* 485:635-641.

681 van der Niet, T., and S. D. Johnson. 2012. Phylogenetic evidence for pollinator-driven
682 diversification of angiosperms. *Trends Ecol Evolut* **27**:353-361.

683 Wagner, G. P., and J. Z. Zhang. 2011. The pleiotropic structure of the genotype-
684 phenotype map: the evolvability of complex organisms. *Nature Reviews Genetics*
685 **12**:204-213.

686 Wessinger, C. A., L. C. Hileman, and M. D. Rausher. 2014. Identification of major
687 quantitative trait loci underlying floral pollination syndrome divergence in
688 *Penstemon*. *Phil. Trans. R. Soc. B* **369**.

689 Wessinger, C. A., C. C. Freeman, M. E. Mort, M. D. Rausher, and L. C. Hileman. 2016.
690 Multiplexed shotgun genotyping resolves species relationships within the North

691 American genus *Penstemon*. *Am J Bot* **103**:912-922.

692 Wessinger, C. A., and J. K. Kelly. 2018. Selfing can facilitate transitions between

693 pollination syndromes. *Am Nat* 191.

694 Wu, M., J. L. Kostyun, M. W. Hahn, and L. C. Moyle. 2018. Dissecting the basis of

695 novel trait evolution in a radiation with widespread phylogenetic discordance.

696 *Mol Ecol* 27: 3301-3316.

697 Wu, M., J. L. Kostyun, and L. C. Moyle. 2019. Genome sequence of *Jaltomata* addresses

698 rapid reproductive trait evolution and enhances comparative genomics in the

699 hyper-diverse Solanaceae. *Genome Biology and Evolution* in press. Available at:

700 https://www.biorxiv.org/content/early/2018/05/30/335117.

701 Xu, S. Q., and P. M. Schluter. 2015. Modeling the two-locus architecture of divergent

702 pollinator adaptation: how variation in SAD paralogs affects fitness and

703 evolutionary divergence in sexually deceptive orchids. *Ecology and Evolution*

704 **5**:493-502.

705

706

707

708

709

710

711

712

713

714 **Table 1**. Summary of measured floral and fertility traits within parental species, F1s, and
715 BC1s. Phenotypic means and variances provided, while significant differences between
716 parental species were assessed with t-tests on transformed data as appropriate (see
717 Methods). Note that significant differences in seed germination rates could not be tested.
718 * p<0.05, ** p<0.001; *** p<0.0001.

| Trait | *J. sinuosa* (n=7) | | *J. umbellata* (n=5) | |
|---|---|---|---|---|
| **Floral Morphology/Physiology** | **Mean** | **Variance** | **Mean** | **Variance** |
| Buds per Inflorescence | *2.86*** | 0.03 | *8.60*** | 3.24 |
| Calyx Diameter (mm) | *15.49*** | 0.08 | *8.14*** | 2.91 |
| Sepal Length (mm) | *7.48*** | 0.02 | *4.41*** | 0.56 |
| Corolla Diameter (mm) | *29.82**** | 1.92 | *15.32**** | 5.70 |
| Corolla Depth (mm) | *1.38*** | 0.07 | *10.25*** | 5.52 |
| Corolla Fusion (mm) | 9.45 | 0.11 | 10.33 | 1.55 |
| Corolla Fusion Proportion | *0.63** | 0.001 | *0.72** | 0.001 |
| Petal Length (mm) | 14.85 | 0.41 | 14.40 | 0.16 |
| Stamen Length (mm) | 10.80 | 0.29 | 10.45 | 0.22 |
| Anther Length (mm) | *2.03** | 0.02 | *1.73** | 0.04 |
| Ovary Diameter (mm) | *2.28**** | 0.03 | *1.37**** | 0.05 |
| Style Length (mm) | *7.90**** | 0.17 | *14.64**** | 1.72 |
| Herkogamy (mm) | *-2.20**** | 0.01 | *5.37**** | 4.62 |
| Nectar Volume (uL) | *6.86**** | 1.07 | *17.80**** | 13.20 |
| **Floral Color** | | | | |
| Nectar Color - Intensity | *205.93**** | 144.59 | *105.59**** | 106.17 |
| Nectar Color - Red | 207.88 | 222.00 | 219.47 | 274.81 |
| Nectar Color - Green | *208.71*** | 148.02 | *66.48*** | 239.95 |
| Nectar Color - Blue | *201.35**** | 105.86 | *30.79**** | 114.53 |
| Nectar Color - Composite RGB | *-202.17**** | 115.02 | *122.20**** | 48.24 |
| Nectar Color - L | *83.49**** | 20.32 | *50.42**** | 31.63 |
| Nectar Color - a | *-1.55**** | 0.95 | *57.61**** | 7.10 |
| Nectar Color - b | *3.47**** | 8.20 | *51.84**** | 59.31 |
| Petal Color - Intensity | *137.05*** | 127.04 | *112.33*** | 136.18 |
| Petal Color - Red | 135.85 | 138.57 | 128.59 | 114.35 |
| Petal Color - Green | 134.31 | 119.92 | 121.87 | 181.62 |
| Petal Color - Blue | *140.97*** | 123.32 | *86.55*** | 134.58 |
| Petal Color - Composite RGB | *-139.42**** | 106.86 | *-79.82**** | 208.17 |
| Petal Color - L | 83.18 | 2.59 | 84.15 | 4.86 |
| Petal Color - a | *0.81** | 0.02 | *-0.93** | 0.62 |
| Petal Color - b | *-1.26**** | 0.02 | *6.71**** | 1.05 |
| **Fertility** | | | | |
| Viable Pollen Grains | 25143 | 36809254 | 26834 | 60773556 |
| Proportion Viable Pollen | 0.76 | 0.01 | 0.71 | 0.02 |
| Fruit Set | *0.93** | 0.01 | *0.55** | 0.06 |
| Fruit Mass (g) | *0.47*** | 0.01 | *0.12*** | 0.01 |
| Fruit Diameter (cm) | *1.01** | 0.01 | *0.61** | 0.02 |

| | | | | |
|---|---|---|---|---|
| Seed Set | *74.87** | 256.92 | *30.44** | 494.43 |
| Viable Seed Set | *74.87** | 256.92 | *23.59** | 182.31 |
| Viable Seed T50 | 9.33 | -- | 7.00 | -- |
| Viable Seed MGT | 22.00 | -- | 14.00 | -- |

**Table 1 cont.**

| F1s (n=13) | | BC1s (n=224) | |
|---|---|---|---|
| **Mean** | **Variance** | **Mean** | **Variance** |
| 3.95 | 0.68 | 3.51 | 1.63 |
| 10.55 | 0.48 | 12.10 | 1.08 |
| 5.45 | 0.13 | 6.16 | 0.28 |
| 24.58 | 6.84 | 28.97 | 9.92 |
| 6.64 | 0.58 | 5.22 | 1.35 |
| 9.81 | 0.40 | 9.92 | 1.24 |
| 0.67 | 0.001 | 0.63 | 0.002 |
| 14.65 | 1.61 | 15.78 | 2.88 |
| 10.81 | 0.59 | 10.86 | 1.26 |
| 2.01 | 0.01 | 2.13 | 0.04 |
| 1.62 | 0.02 | 1.82 | 0.04 |
| 12.39 | 1.04 | 10.82 | 1.97 |
| 2.95 | 1.08 | 1.20 | 1.02 |
| 11.90 | 12.32 | 10.76 | 18.87 |
| 172.44 | 110.66 | 192.70 | 272.74 |
| 232.93 | 149.55 | 213.14 | 127.46 |
| 198.03 | 248.93 | 206.89 | 165.90 |
| 74.27 | 317.30 | 157.76 | 1591.28 |
| -39.37 | 1182.31 | -151.51 | 2429.74 |
| 81.31 | 14.35 | 83.99 | 13.42 |
| -0.05 | 101.74 | -4.29 | 14.91 |
| 59.85 | 75.94 | 22.91 | 287.97 |
| 147.02 | 63.03 | 135.30 | 119.75 |
| 152.60 | 100.19 | 137.00 | 144.35 |
| 154.91 | 246.30 | 135.92 | 138.89 |
| 137.41 | 105.01 | 132.70 | 113.98 |
| -139.72 | 391.57 | -131.62 | 142.13 |
| 86.93 | 5.82 | 83.56 | 4.60 |
| -0.81 | 0.19 | -0.04 | 0.36 |
| 2.89 | 3.13 | 0.75 | 1.29 |
| 22513 | 16602405 | 26886 | 145318716 |
| 0.82 | 0.00 | 0.74 | 0.03 |
| 0.93 | 0.01 | 0.89 | 0.03 |
| 0.24 | 0.01 | 0.29 | 0.01 |
| 0.80 | 0.01 | 0.85 | 0.03 |
| 36.06 | 168.37 | 37.67 | 361.12 |
| 25.46 | 303.95 | 26.28 | 340.08 |
| 34.00 | 1001.78 | 26.70 | 607.37 |
| 46.04 | 622.37 | 39.36 | 458.11 |

721 **Table 2**. Summary of identified QTL for key floral and fertility traits. Includes peak
722 location and LOD of QTL, 1.5 LOD intervals, amount of phenotypic variance of trait
723 explained, phenotypic effect size and standard error (back-transformed where applicable),
724 and whether the effect is aligned with parental trait values. Full QTL data, including the
725 full models for all traits, are provided in Table S6.

| Trait Category | Trait | LG | Peak Location | Peak LOD |
|---|---|---|---|---|
| Flower Morph | Inflor. Size (2) | LG 4 | 55.4 | 3.04 |
| | | LG 1 | 56 | 3.02 |
| | Calyx Dia (3) | LG 1 | 56 | 9.06 |
| | | LG 8 | 84.3 | 3.15 |
| | | LG 9 | 66 | 5.59 |
| | Sepal Length (3) | LG 1 | 57 | 8.30 |
| | | LG 12 | 23 | 3.74 |
| | | LG 9 | 65.9 | 7.04 |
| | Corolla Dia (3) | LG 4 | 21.1 | 3.50 |
| | | LG 12 | 37.4 | 1.57 |
| | | LG 8 | 73.1 | 5.87 |
| | Corolla Depth (4) | LG 7 | 52 | 17.95 |
| | | LG 5 | 40.8 | 10.19 |
| | | LG 10 | 55.8 | 4.48 |
| | | LG 9 | 30 | 12.38 |
| | Corolla Fusion Prop (4) | LG 5 | 86 | 3.57 |
| | | LG 4 | 26 | 3.77 |
| | | LG 1 | 72 | 4.60 |
| | | LG 9 | 16 | 7.19 |
| | Petal Length (3) | LG 7 | 100 | 2.46 |
| | | LG 12 | 48.2 | 2.04 |
| | | LG 8 | 73 | 3.55 |
| | Stamen Length (4) | LG 7 | 91 | 4.45 |
| | | LG 4 | 120.8 | 3.77 |
| | | LG 2 | 37.5 | 4.54 |
| | Anther Length (1) | LG 9 | 0 | 5.32 |
| | | LG 1 | 18 | 3.78 |
| | Ovary Dia (4) | LG 7 | 9.9 | 3.56 |
| | | LG 5 | 72 | 2.53 |

| | | | | |
|---|---|---|---|---|
| | Style Length (2) | LG 1 | 68 | 5.77 |
| | | LG 12 | 48.2 | 4.31 |
| | | LG 2 | 95.2 | 2.79 |
| | | LG 9 | 22 | 9.89 |
| | Herkogamy (5) | LG 1 | 314 | 4.53 |
| | | LG 2 | 112 | 7.26 |
| | | LG 11 | 40 | 4.79 |
| | | LG 8 | 51.4 | 3.27 |
| | | LG 9 | 7.3 | 4.32 |
| | PC1 (6) | LG 5 | 116 | 3.61 |
| | | LG 4 | 59.2 | 3.55 |
| | | LG 1 | 54.2 | 4.08 |
| | | LG 2 | 31.7 | 4.73 |
| | | LG 8 | 82 | 8.08 |
| | | LG 9 | 19 | 10.34 |
| | PC2 (3) | LG 1 | 58 | 2.62 |
| | | LG 12 | 48.2 | 3.27 |
| | | LG 8 | 58 | 2.14 |
| | PC3 (2) | LG 1 | 67.5 | 4.99 |
| | | LG 9 | 24.7 | 11.52 |
| Flower Physio | Nectar Volume (1) | LG 3 | 187.2 | 2.81 |
| | Nectar PC1 (3) | LG 7 | 28 | 9.91 |
| | | LG 5 | 100 | 13.15 |
| | | LG 2 | 153 | 5.48 |
| | Nectar PC2 (1) | LG 7 | 8.4 | 3.29 |
| Flower Color | Nectar PC3 (1) | LG 3 | 66.1 | 3.47 |
| | Petal PC1 (1) | LG 5 | 65.3 | 5.83 |
| | Petal PC2 (2) | LG 5 | 63 | 18.91 |
| | | LG 9 | 67 | 10.42 |
| | Petal PC3 (0) | no QTL | | |
| | Fruit Set (0) | no QTL | | |
| | Fruit Dia (2) | LG 1 | 80 | 4.67 |
| | | LG 11 | 76.9 | 3.09 |
| Fertility | Fruit Mass (4) | LG 3 | 170 | 2.67 |
| | | LG 1 | 96 | 5.47 |
| | | LG 11 | 76.5 | 5.63 |
| | | LG 12 | 0 | 4.51 |
| | Seed Set (2) | LG 11 | 76 | 6.64 |
| | | LG 12 | 0 | 2.86 |
| | Viable Seed Set (1) | LG 11 | 76.9 | 4.42 |
| | Viable Pollen (0) | no QTL | | |

727 **Table 2 cont.**

| 1.5 LOD Intervals | %PVE | Effect | Effect SE | Aligned with Parental Value? |
|---|---|---|---|---|
| 15-108 | 5.50 | 1.1576 | 0.0169 | YES |
| 34-133 | 5.46 | -1.1628 | 0.0175 | NO |
| 49-81 | 13.67 | -0.8026 | 0.1202 | YES |
| 69-92.55 | 4.46 | -0.4565 | 0.1196 | YES |
| 17-85 | 8.13 | -0.5976 | 0.1160 | YES |
| 49-70.73 | 12.17 | -0.3923 | 0.0616 | YES |
| 10-59 | 5.22 | -0.2539 | 0.0609 | YES |
| 22-73 | 10.18 | -0.3404 | 0.0584 | YES |
| 13-70 | 4.47 | 1.3869 | 0.3440 | NO |
| 0-65.17 | 1.96 | -0.9630 | 0.3606 | YES |
| 67-84 | 7.69 | -1.9019 | 0.3596 | YES |
| 48-60.67 | 21.47 | 1.1455 | 0.1164 | YES |
| 20-46 | 11.20 | 0.8437 | 0.1187 | YES |
| 41-91 | 4.64 | -0.5214 | 0.1140 | NO |
| 11-38 | 13.94 | 0.9420 | 0.1188 | YES |
| 80.21-99 | 5.39 | 0.0005 | 0.0000 | YES |
| 19-84 | 5.70 | -0.0004 | 0.0000 | NO |
| 57-106 | 7.02 | -0.0005 | 0.0000 | NO |
| 0-67 | 11.27 | 0.0008 | 0.0000 | YES |
| 25-100.67 | 3.29 | 1.0414 | 0.0050 | NO |
| 0-65.17 | 2.71 | 1.0390 | 0.0053 | YES |
| 39-92.55 | 4.78 | -1.0657 | 0.0053 | YES |
| 59-100.67 | 5.68 | 0.5510 | 0.1209 | NO |
| 100-133 | 4.78 | -0.4994 | 0.1194 | YES |
| 6-61 | 5.80 | -0.5478 | 0.1190 | YES |
| 0-33 | 6.86 | 0.6194 | 0.1237 | NO |
| 8-35.87 | 6.48 | -0.1157 | 0.0274 | YES |
| 0-25 | 5.56 | -0.0936 | 0.0230 | YES |
| 0-84 | 3.90 | 0.0915 | 0.0269 | NO |
| 60-107 | 9.21 | -0.1196 | 0.0229 | YES |
| 5-65.17 | 6.78 | -0.1036 | 0.0231 | YES |
| 55-126 | 3.80 | 1.0517 | 0.0061 | YES |
| 1-30 | 14.51 | 1.1072 | 0.0063 | YES |
| 266-324 | 6.42 | -1.1613 | 0.0141 | NO |
| 30-122 | 10.60 | 1.2156 | 0.0144 | YES |
| 5-63 | 6.81 | 1.2143 | 0.0783 | YES |
| 26-63 | 4.57 | 1.1344 | 0.0141 | YES |

| | | | | |
|---|---|---|---|---|
| 3.47-32 | 6.12 | 1.1560 | 0.0140 | YES |
| 95-124.77 | 3.61 | 0.3880 | 0.1025 | YES |
| 24-76 | 3.55 | -0.3691 | 0.0983 | NO |
| 34-86 | 4.08 | 0.3853 | 0.0958 | YES |
| 4-44 | 4.73 | 0.4121 | 0.0952 | YES |
| 68.51-92.55 | 8.08 | 0.5552 | 0.0981 | YES |
| 12-71 | 10.34 | 0.6040 | 0.0943 | YES |
| 43-138 | 3.72 | -0.6666 | 0.1921 | YES |
| 16-62.42 | 4.69 | -0.7556 | 0.1940 | YES |
| 36-92.55 | 3.03 | -0.6066 | 0.1939 | YES |
| 46-86 | 7.27 | -0.6665 | 0.1371 | YES |
| 20-31 | 18.01 | -1.0720 | 0.1401 | YES |
| 172-187.19 | 5.22 | 1.2539 | 0.0366 | YES |
| 23-37 | 11.96 | -1.5076 | 0.2152 | YES |
| 83-107 | 16.45 | -1.9822 | 0.2413 | YES |
| 147-171.87 | 6.31 | -1.1060 | 0.2174 | YES |
| 0-22 | 6.21 | 0.7061 | 0.1801 | NO |
| 17-121 | 6.92 | -0.5691 | 0.1412 | YES |
| 60-72 | 11.4 | -1.7713 | 0.3344 | YES |
| 59-67 | 28.06 | -1.4839 | 0.1453 | YES |
| 39.15-73 | 14.09 | -0.9231 | 0.1276 | YES |
| | | | | |
| 61-103 | 8.64 | -1.0608 | 0.0054 | YES |
| 51-79.93 | 5.61 | -1.0463 | 0.0052 | YES |
| 48-187.19 | 4.07 | -1.0168 | 0.0023 | YES |
| 60-146 | 8.58 | -0.9745 | 0.0049 | YES |
| 54-79.93 | 8.85 | -0.9762 | 0.0047 | YES |
| 0-10.64 | 7.01 | -0.9771 | 0.0050 | YES |
| 63-79.93 | 12.28 | -1.4353 | 0.0277 | YES |
| 0-63 | 5.07 | -1.2857 | 0.0300 | YES |
| 68-79.93 | 8.85 | -1.6267 | 0.0462 | YES |

728

729

730

731

732

733

734 **Figure Legends.**

735 **Figure 1**. Representative flowers of the parental species and their F1 hybrid.

736

737 **Figure 2**. Key trait distributions within the BC1 population, compared to phenotypic

738 means for *J. sinuosa* (purple line), *J. umbellata* (red line), and their F1s (pink line).

739

740 **Figure 3**. Key floral trait correlations within the BC1 mapping population. Scatterplots

741 are provided below the diagonal, while Spearman's correlation coefficients and

742 associated p-values are above the diagonal. Statistically significant correlations following

743 Bonferroni correction ($p < 3.125 \times 10^{-5}$) are highlighted in red. Correlation values for all

744 traits are provided in Table S3, and for PC traits provided in Table S5.

745

746 **Figure 4**. Linkage map and distribution of identified QTL (including 1.5 LOD intervals)

747 for 12 key floral and fertility traits.

748

749

750 **Supplementary Information**

751 **Table S1.** Accession information for material used and generated in this study.

752 **Table S2**. Trait measurements for all individuals phenotyped in this study.

753 **Table S3**. Correlations among all measured traits within BC1 individuals.

754 **Table S4**. Principle component loadings for highly correlated traits.

755 **Table S5**. Correlations among PC traits within BC1 individuals

756 **Table S6**. Full QTL models for all examined traits.

**Table S7**. Expected and observed counts of QTL overlap.

**Figure S1**. Measured morphological traits on mature flowers.

**Figures S2-S3**: Distributions for floral morphological and physiological traits within the mapping population.

**Figure S4**. Distributions for nectar color traits within the mapping population.

**Figure S5**. Distributions for petal color traits within the mapping population.

**Figure S6**. Distributions for fertility traits within the mapping population.

**Figure S7**. Representative examples of petal color variation among F1 individuals, compared to either parent.

**Figure S8**. Comparison of observed number of QTL overlaps with counts from 10000 randomly generated simulations, for QTL co-localization overlap within and between trait categories (morphology, color, and fertility).


J. sinuosa
F1
J. umbellata
1 cm

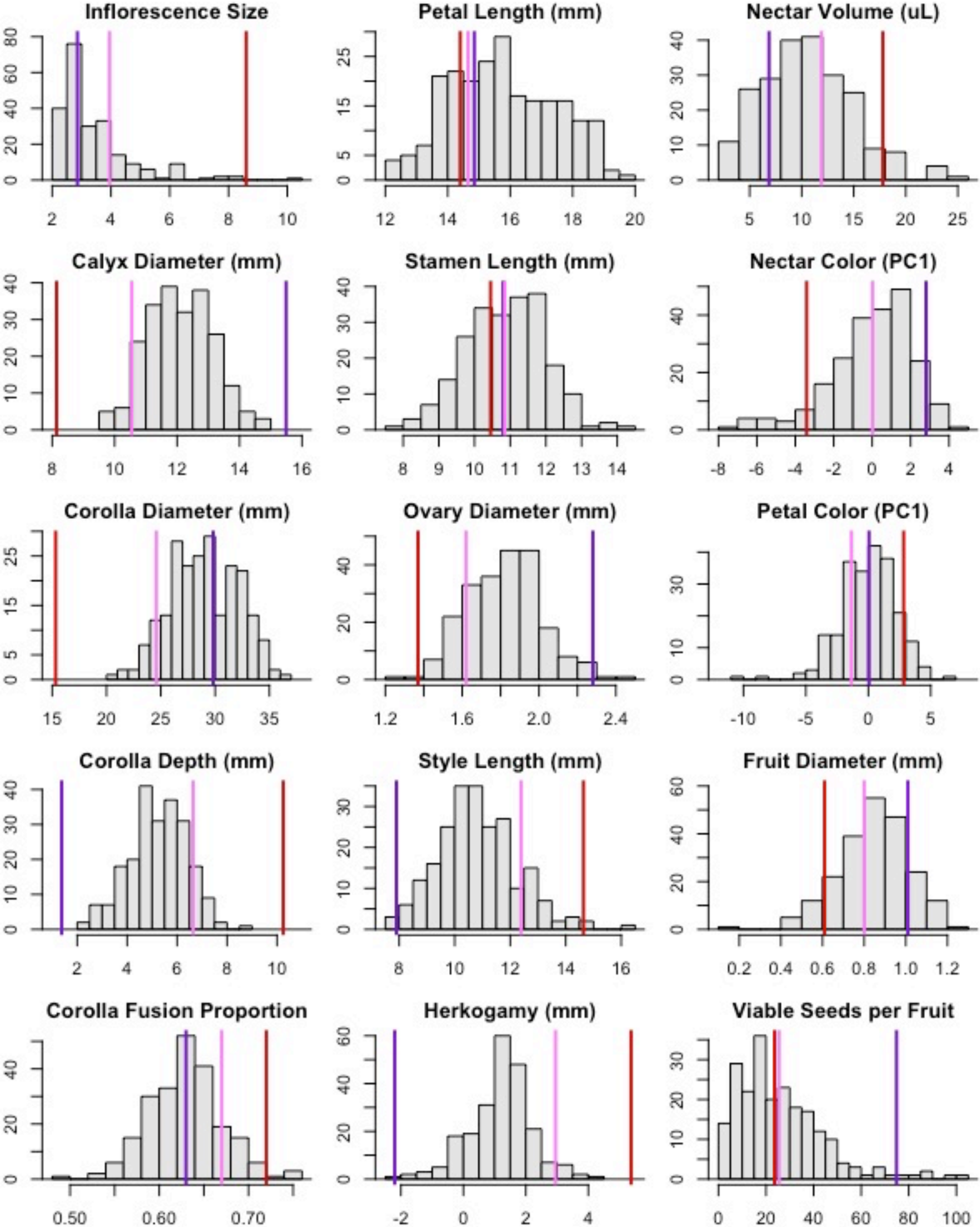
Inflorescence Size
Petal Length (mm)
Nectar Volume (uL)
Calyx Diameter (mm)
Stamen Length (mm)
Nectar Color (PC1)
Corolla Diameter (mm)
Ovary Diameter (mm)
Petal Color (PC1)
Corolla Depth (mm)
Style Length (mm)
Fruit Diameter (mm)
Corolla Fusion Proportion
Herkogamy (mm)
Viable Seeds per Fruit

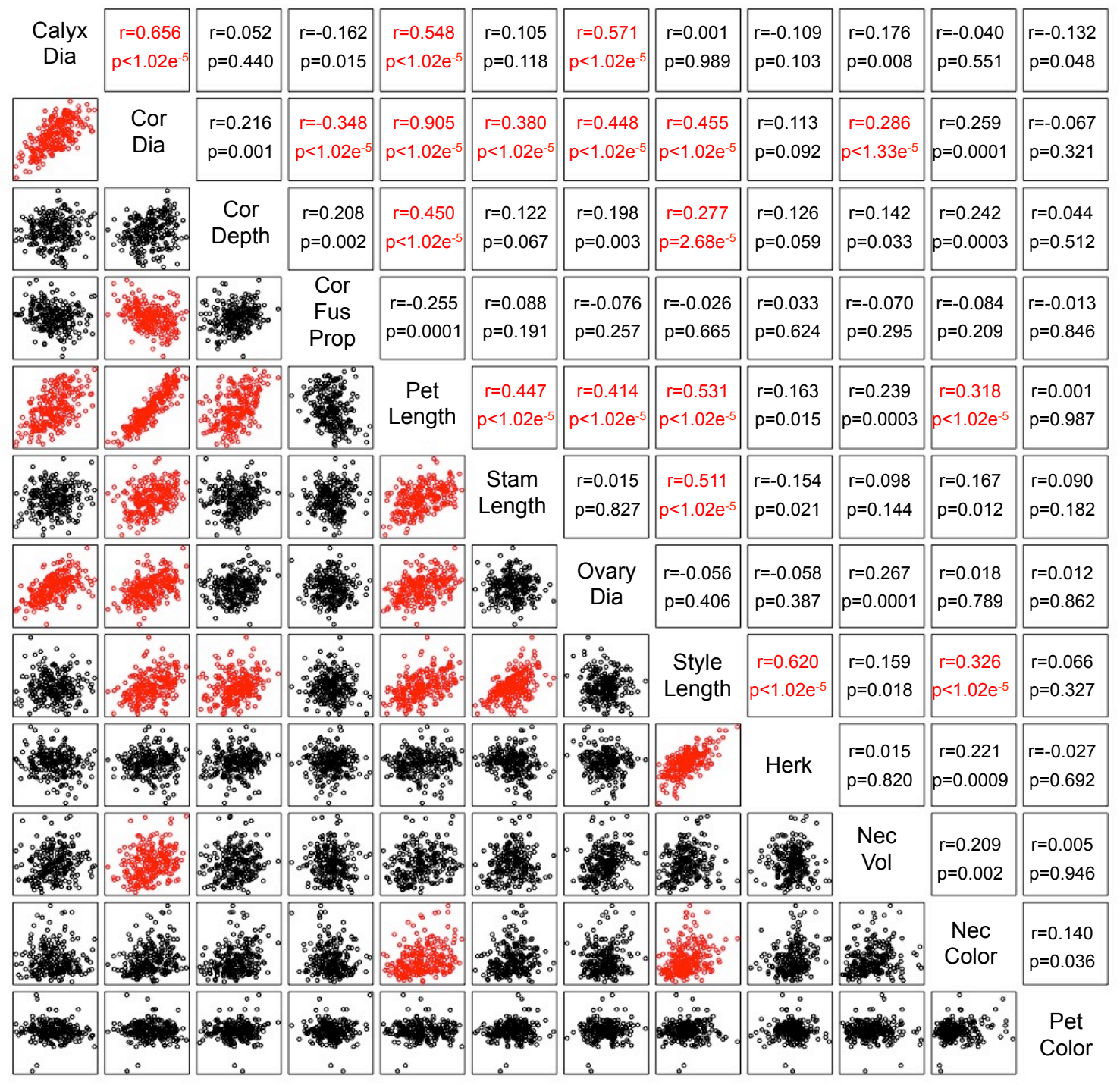
Calyx Dia
r=0.656 p<1.02e-5
r=0.052 p=0.440
r=-0.162 p=0.015
r=0.548 p<1.02e-5
r=0.105 p=0.118
r=0.571 p<1.02e-5
r=0.001 p=0.989
r=-0.109 p=0.103
r=0.176 p=0.008
r=-0.040 p=0.551
r=-0.132 p=0.048
Cor Dia
r=0.216 p=0.001
r=-0.348 p<1.02e-5
r=0.905 p<1.02e-5
r=0.380 p<1.02e-5
r=0.448 p<1.02e-5
r=0.455 p<1.02e-5
r=0.113 p=0.092
r=0.286 p<1.33e-5
r=0.259 p=0.0001
r=-0.067 p=0.321
Cor Depth
r=0.208 p=0.002
r=0.450 p<1.02e-5
r=0.122 p=0.067
r=0.198 p=0.003
r=0.277 p=2.68e-5
r=0.126 p=0.059
r=0.142 p=0.033
r=0.242 p=0.0003
r=0.044 p=0.512
Cor Fus Prop
r=-0.255 p=0.0001
r=0.088 p=0.191
r=-0.076 p=0.257
r=-0.026 p=0.665
r=0.033 p=0.624
r=-0.070 p=0.295
r=-0.084 p=0.209
r=-0.013 p=0.846
Pet Length
r=0.447 p<1.02e-5
r=0.414 p<1.02e-5
r=0.531 p<1.02e-5
r=0.163 p=0.015
r=0.239 p=0.0003
r=0.318 p<1.02e-5
r=0.001 p=0.987
Stam Length
r=0.015 p=0.827
r=0.511 p<1.02e-5
r=-0.154 p=0.021
r=0.098 p=0.144
r=0.167 p=0.012
r=0.090 p=0.182
Ovary Dia
r=-0.056 p=0.406
r=-0.058 p=0.387
r=0.267 p=0.0001
r=0.018 p=0.789
r=0.012 p=0.862
Style Length
r=0.620 p<1.02e-5
r=0.159 p=0.018
r=0.326 p<1.02e-5
r=0.066 p=0.327
Herk
r=0.015 p=0.820
r=0.221 p=0.0009
r=-0.027 p=0.692
Nec Vol
r=0.209 p=0.002
r=0.005 p=0.946
Nec Color
r=0.140 p=0.036
Pet Color

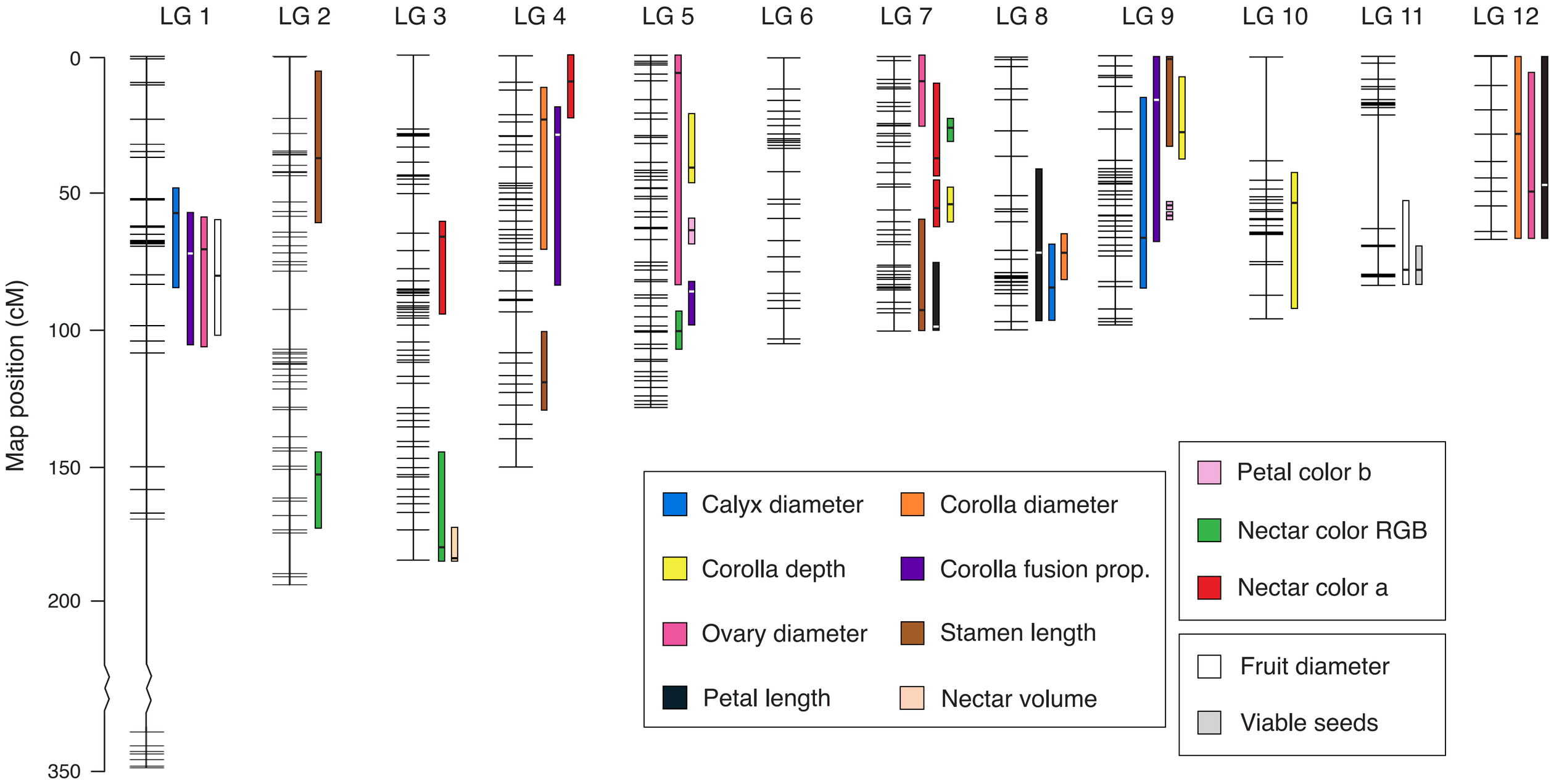
LG 1
LG 2
LG 3
LG 4
LG 5
LG 6
LG 7
LG 8
LG 9
LG 10
LG 11
LG 12
Map position (cM)
0
50
100
150
200
350
Calyx diameter
Corolla diameter
Corolla depth
Corolla fusion prop.
Ovary diameter
Stamen length
Petal length
Nectar volume
Petal color b
Nectar color RGB
Nectar color a
Fruit diameter
Viable seeds